Evaluating the Effect of using different filters in Thyroid SPECT Image Reconstruction.

H.I.AbdelKader[1], H.Gad[2], Omneya Foda[3]

Abstract: In nuclear medicine, thyroid disorders is diagnosed using single photon emission computed tomography (SPECT) imaging. Noise reduction is one of the important tasks in SPECT imaging. In this study thyroid of thirty patients was imaged using gamma camera. Images in the transaxial direction were reconstructed by order subset expectation maximization (OSEM) technique. Five digital filters (Butterworth, Hamming, Hanning, Metz and Wiener) were used for reducing noise. The aim of this study is to evaluate the optimum parameter for each filter to obtain the best physical image parameters (Resolution, Contrast and Noise). The optimum parameter of each filter is as following: for Butterworth filter (cutoffs 0.2, 0.4) with (order 5) and (orders 2, 4) with (cutoff 0.5), for Hamming filter (alpha 0.5), for Hanning filter (cutoff 0.5), for Metz filter full width at half maximum (FWHM 6, 8) with (order 5), for Wiener filter (FWHM 8). These are the best parameters for the five filters that produce high quality images, which in turn help the physicians come up with the best and most accurate diagnosis of thyroid disorders.

Keywords: Thyroid SPECT, Gamma camera, Image reconstruction, Digital filters, Butterworth, Hamming filter, Hanning filter , Metz , Weiner filter

1-Associate Prof .Physics department, faculty of science
Mansoura University .Email: hikader5@yahoo.com
2-Prof.Mansoura Urology and Nephrology Center, faculty of medicine
Mansoura University.
3- MSC Research Student, Faculty of science
Mansoura University, omneyafoda@gmail.com

1 Introduction:

Thyroid gland is a part of the body's endocrine system that excretes hormones which are important for regulatory functions. Nuclear medical imaging plays an important role in determining thyroid function which is helping in diagnosis, characterization or localization of many disorders. Nuclear medicine tomography is a noninvasive imaging technique that is used to generate cross-sectionals images of a three dimensional (3D) object without superimposing tissues. Tomography can be categorized in transmission tomography such as computed tomography (CT) and emission tomography like single photon emission computed tomography (SPECT) and positron emission tomography (PET). Single photon emission computed tomography (SPECT) provides 3D image information about the radionuclide injected into the patient that shows the metabolic and physiological activities within an organ [1].

In tomographic techniques, projections are acquired from many different angles around the body by one or more rotating detectors. These data are then reconstructed and put together to form 3D images of the body. The reconstruction of tomographic images is made by two methods: filtered backprojection (FBP) and iterative methods like ordered subset expectation maximization (OSEM) [2].

One of the important tasks in clinical single photon emission computed tomography (SPECT) imaging is noise reduction; therefore different digital filters have been suggested. Butterworth, Metz, Hamming, Hanning , and Wiener filters are commonly used in SPECT during OSEM reconstruction. The quality and accuracy of the image are greatly affected by applying these filters [3].

The quality of the final tomographic image is limited by several factors. Some of these are the attenuation and scatter of gamma ray photons, the detection efficiency and the spatial resolution of the collimator-detector system [3].

These factors have as a result poor spatial resolution, low contrast, and high noise levels. Image filtering techniques are very important in tomography as they strongly affect the quality of the image. Image filtering is the term used for any operation that is applied to pixels in an image. It is a mathematical process by which images are suppressed in noise and also includes smoothing, edge enhancement and resolution recovery. Filters are used during reconstruction and applied to data in frequency domain. The goal of the filtering is to compensate for loss of detail in an image while reducing noise [4].

The criterion which we have used in judging the performance of a filter function is in terms of its effect on the physical parameters of the image: resolution, contrast and noise [5]. All filters fall into one of three classes: (1) Low-Pass filters (filters that pass low frequencies), (2) High-Pass filters (filters that pass high frequencies), and (3) Band-Pass filters (filters that pass a narrow range of frequencies). The goal of applying filters in nuclear medicine is to reduce this noise, which means low-pass filters are mostly employed. There are many Low-Pass filters that could be used including Butterworth , Metz , Weiner , Hanning and Hamming [6].

The purpose of this study is to evaluate the optimum parameter for each filter to obtain the best physical image parameters (Resolution, Contrast and Noise).

2 Subjects and Methods:

The study was carried in Urology and Nephrology Center in Mansoura University after obtaining approval of Mansoura ethic community. Informed consents were also obtained from all participating subjects after explanation of the study was given to the participating. Inclusion criteria for study were thyroid disorders. The study included 30 patient (12 male and 18 female) aged between 40-65 years.

Gamma camera used in this study was Toshiba DST-Xli. This camera has dual detectors, each detector head housed the NaI(TL) crystal and 94 photomultiplier tubes (PMTs). The SPECT tomography was applied using parallel low energy high resolution collimator. ^{99m}Tc-sestamibi was injected to the patient, having gamma energy of 140 Kev of ^{99m}Tc and half-life of 6.02 hours. Thirty patients with thyroid disorders are selected randomly and examined for SPECT study.

Tomographic acquisitions were performed using the following parameters: 128*128 pixels, matrix size with pixel size 4.51*4.51 mm^2, magnification = 2. Number of views was 128 which were obtained by step and shot rotation mode of the gamma camera detector head. Time per acquisition was 20 sec. Reconstruction matrix was 128*128 pixels. Transverse slices were reconstructed by OSEM (ordered subset expectation maximization) algorithm at subset number 8 and 2 iterations.

2.1 Filters:

Five low pass filters were applied on reconstructed images including: Butterworth, Hanning, Hamming, Metz and Wiener filters.

Butterworth Filter

Butterworth filter is the more usual choice in nuclear medicine. The Butterworth filter is a low pass filter. It is characterized by two parameters: the critical frequency which is the point at which the filter starts its roll-off to zero and the order or power [6]. The order changes the slope of the filter. Because of this ability of changing not only the critical frequency but also the steepness of the roll-off, the Butterworth filter can do both, smoothies noise and preserves the image resolution.
A Butterworth filter in spatial domain is described by the following equation (1) and figure (1):

$$\mathrm{B}(f) = \frac{}{[1+(f/f_c)]^{2n}} \qquad (1)$$

where (f) is the spatial frequency domain, (f_c) is the critical frequency and (n) is the order of the filter.

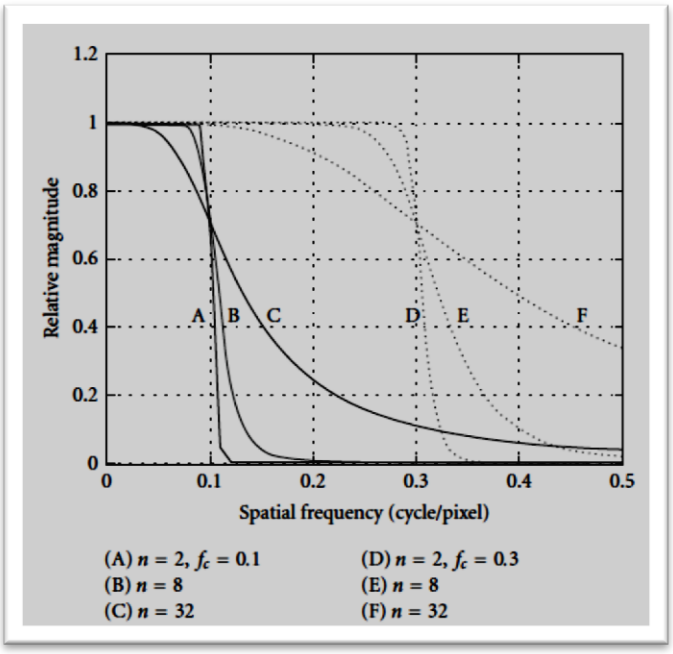

Figure (1) Butterworth smoothing filter six curves by different (f_c) and (n) parameters (equation (1)). A, B, C curves created by critical frequency (f_c = 0.1 c/pixel) and order (n) equal to 2, 8, 32 correspondingly. D, E, F curves created by critical frequency (f_c = 0.3 c/pixel) and order (n) equal to 2, 8, 32 similarly [6].

Hanning Filter

Hanning filter is a relatively simple low-pass filter which is described by one parameter, the cut-off (critical) frequency (Figure 2) [7]. Hanning filter is defined in the frequency domain as shown in the following equation (2):

$$\mathrm{H}(f) = \begin{cases} 0.5 + 0.5\cos\left(\frac{\pi f}{f_m}\right), & 0 \le |f| \le f_m, \\ 0, & \end{cases} \qquad (2)$$

where (f) are the spatial frequencies of the image and (f_m) the cut-off (critical) frequency.

In signal processing, the Hann window is a window function, called the Hann function, named after Julius Ferdinand von Hann, an Austrian meteorologist. The use of the Hann window is called "Hanning", as a signal to apply the Hann window to a digital signal processing. The Hanning (Hann) filter is very effective in reducing image noise as it reaches zero very quickly; however, it does not preserve edges (Figure 2).

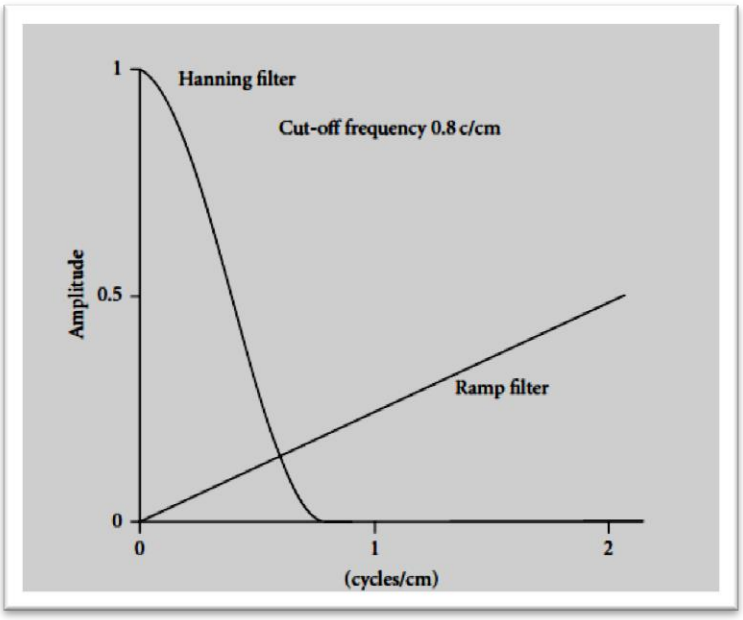

Figure (2) Hanning filter and Ramp in FBP reconstruction.

Hamming Filter

Hamming filter is also a low-pass filter, which presents a high degree of smoothing, named after Richard Wesley Hamming, an American mathematician famous in computer science. As the Hanning filter, it has only a single parameter to describe its shape, the cut-off frequency. The mathematical definition is shown in the following equation (3):

$$\mathrm{H}(f) = \begin{cases} 0.54 + 0.46\cos\left(\frac{\pi f}{f_m}\right), & 0 \le |f| \le f_m, \\ 0, \end{cases} \qquad (3)$$

where (f) is the spatial frequency of the image and (f_m) is the cut-off frequency. As it can be observed the only difference with the Hanning filter is on the amplitude at the cut-off frequency [7].

Metz Filter

Metz filter is a function of modulation transfer function (MTF), and it is based on the measured MTF of the gamma camera system. The MTF describes how the system handles or degrades the frequencies. The Metz restoration filter is defined in the frequency domain as shown in the following equation (4):

$$\mathrm{M}(f) = \mathrm{MTF}(f)^{-}\ [\mathrm{l} -\ (\mathrm{l} - \mathrm{MTF}(f)^2)^x], \qquad (4)$$

where (f) is the spatial domain and is a parameter that (x) controls the extent to which the inverse filter is followed before the low-pass filter rolls off to zero [8]. Equation (4) is the product of the inverse filter

(first term) and a low pass filter (second term). The Metz filter is count dependent. Figure (3) shows the Metz filter plotted for six different total image counts. From Figure (3) results that, as the counts increase, more resolution recovery occurs (filter rises farther above 1.0), together with less suppression (filter moves farther to right) [9].

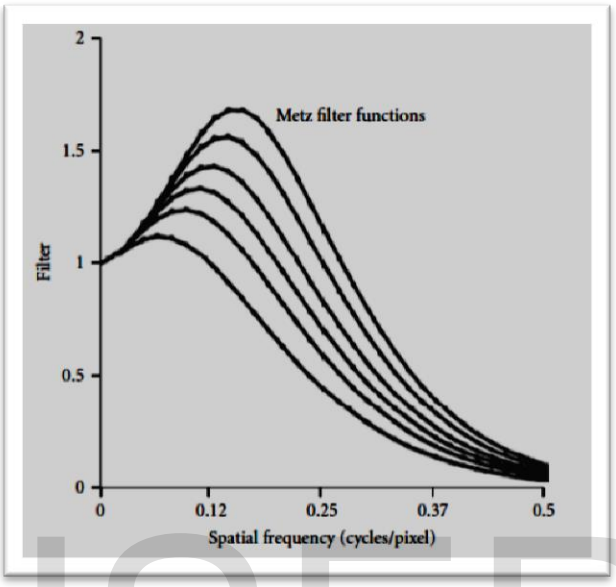

Figure (3) Plot of Metz filter for total counts of 20.000, 50.000, 100.000, 200.000, 500.000, and 1 million counts from lowest to highest curve.

Wiener filter

Wiener filter is based on the signal-to-noise ratio (SNR) of the specific image. The one dimensional frequency domain form of the Wiener filter is defined in the following equation (5):

$$W(f) = \mathrm{MTF}^{-1} \times \frac{\mathrm{MTF}^2}{(\mathrm{MTF}^2 + \mathrm{N/O})}, \qquad (5)$$

where (MTF) is the modulation transfer function of the imaging system, (N) is the noise power spectrum, and (O) is the object power spectrum [10]. As with the Metz filter, the Wiener is the product of the inverse filter (which shows the resolution recovery) and the low pass filter (which shows the noise suppression). In order to apply the Wiener filter it is necessary to know a priori the MTF, the power spectrum of the object and the power spectrum of the noise. It has to be noted that is, impossible to know exactly the MTF or the SNR (signal-to-noise ratio) in any image. As a result, the mathematical models used to optimize both Metz and Wiener filters are uncertain [11].

2.2 Data analysis:

The images were analyzed after reconstruction and filtering. Three important parameters affect the quality of the image: Resolution, Contrast and Noise.

Resolution

Resolution (spatial resolution) is that distance, which is between two points that are just separable after the image reconstruction. There is another definition of spatial resolution: it can be expressed by the full width at half maximum (FWHM) of the line spread function (LSF) [6]. FWHM was calculated by drawing a vertical line profile cutting the left lobe of the thyroid and applying it in the origin-Pro(8) program in the computer, while (x –axis represent the pixels of the image ,y-axis representing the count).

Contrast

Contrast is defined as the differences in image density (or intensity) between adjacent areas (pixels) in the image, containing different concentrations of radioactivity [12]. It was calculated by determining a region of interest (ROI) in the left lobe of the imaged thyroid gland. Contrast was given in equation (6):

$$C\% = 100 \times (C_{ROI} - C_{bk}) / (C_{ROI} + C_{bk}), \quad (6)$$

where (C_{ROI}) is the counts in the ROI through the targeted area of the imaged organ and (C_{bk}) is the counts in the background for the same area of pixels.

Image Noise

Image noise is caused by random fluctuations in radioactive decay process as well as statistical uncertainties that arise during imaging with gamma camera. For these reasons nuclear medicine images contain statistical variations on noise [13]. Noise was measured by drawing a region of interest in the left lobe of the thyroid gland. The mean and standard deviation (SD) within the ROI were measured and the percent root mean square noise (RMS) was calculated from equation (7):

$$\%RMS = 100 \times SD/mean, \quad (7)$$

3 Results and Discussion:

The results of this study can have important clinical applications. SPECT filters can greatly affect the quality of clinical images by their degree of smoothing. Determining the best filter and the proper degree of smoothing can help to ensure the most accurate diagnosis. These results can also help to speed image processing time since a proper filter function is often chosen clinically by the tedious and time-consuming process of trial and error.

3.1 Results:

Images (with 4 frames) with different filter parameters were collected together to represent the difference visually for the physician as shown in the following figures. Then frame 15 in each image was analyzed to evaluate resolution, contrast and noise.

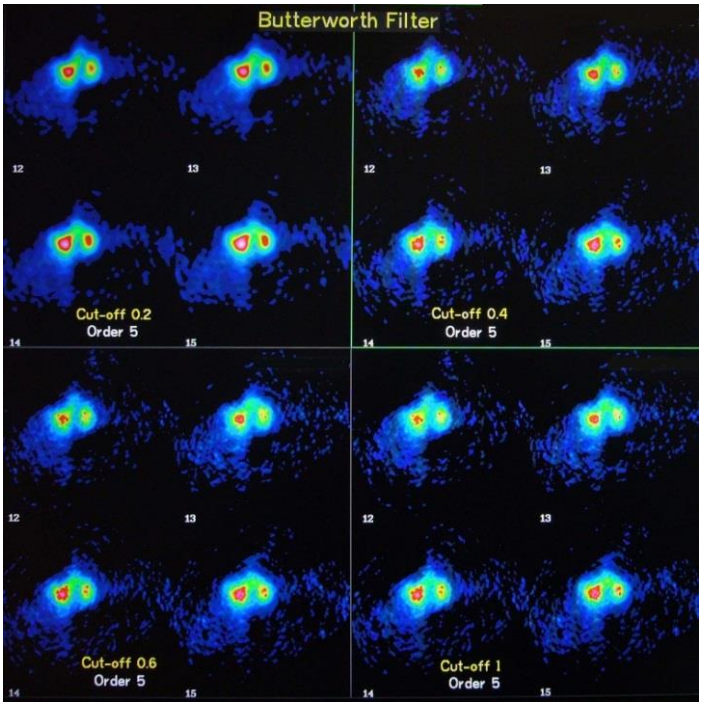

Figure (4) Transverse thyroid frames, reconstructed by OSEM. Butterworth filter was applied after reconstruction, with four different cut-offs (0.2, 0.4, 0.6, 1 cm^{-1}) with fixed order 5.

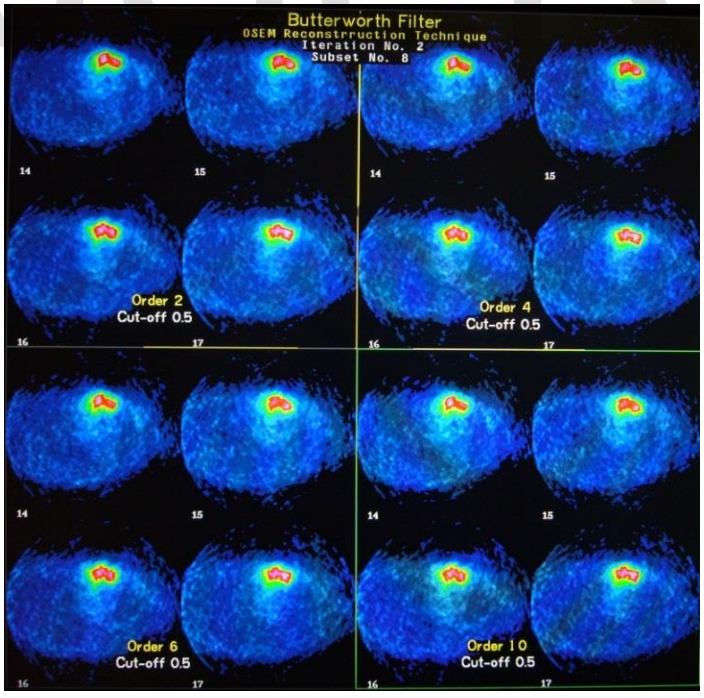

Figure (5) Transverse thyroid frames, reconstructed by OSEM. Butterworth filter was applied after reconstruction, with four different orders (2, 4, 6, 10) with fixed cut-off 0.5 cm^{-1}.

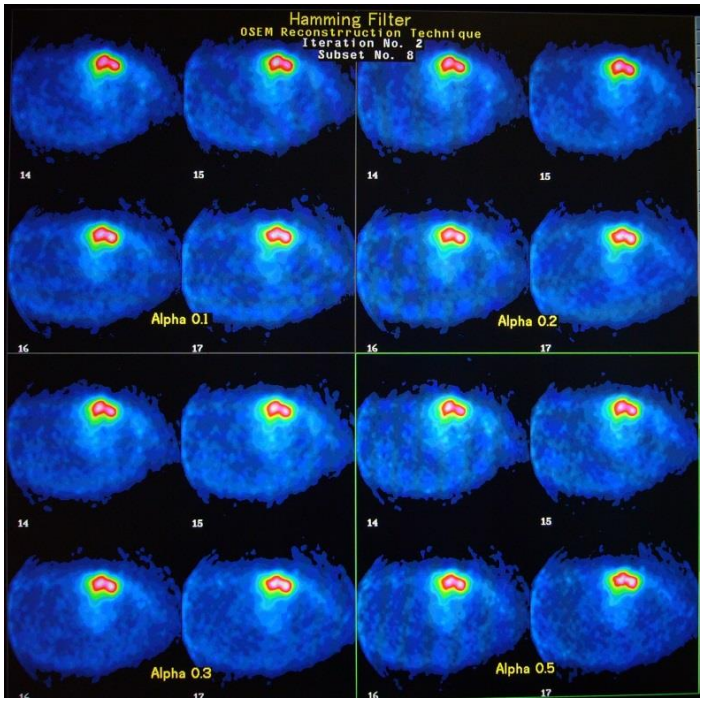

Figure (6) Transverse thyroid frames, reconstructed by OSEM. Hamming filter was applied after reconstruction, with four different parameters of Alpha (0.2, 0.4, 0.3, 0.5 cm^{-1}) .

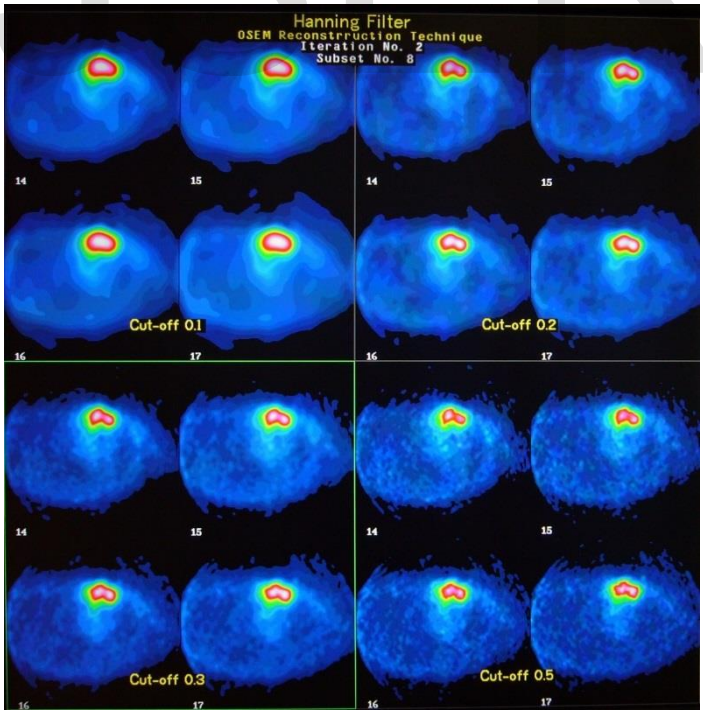

Figure (7) Transverse thyroid frames, reconstructed by OSEM. Hanning filter was applied after reconstruction, with four different cut-offs (0.2, 0.4, 0.3, 0.5 cm^{-1}).

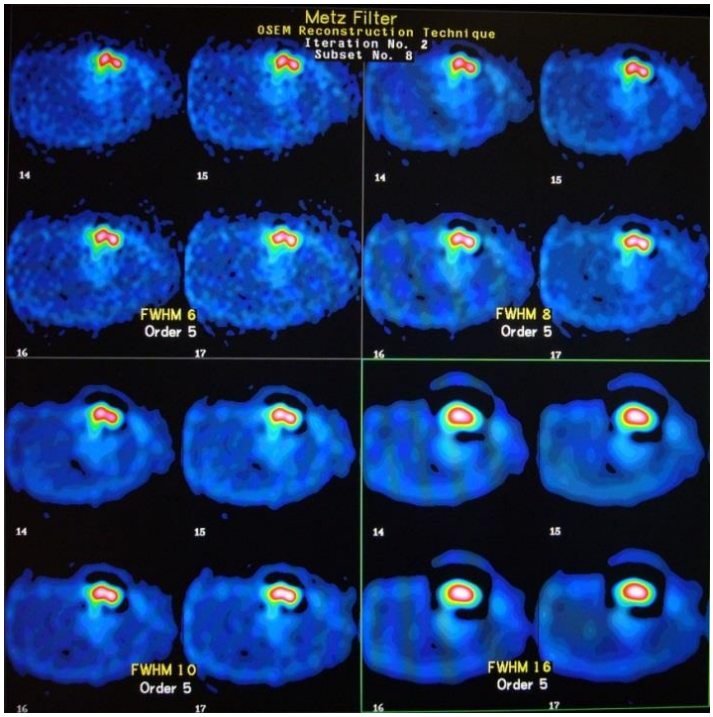

Figure (8) Transverse thyroid frames, reconstructed by OSEM .Metz filter was applied after reconstruction, with four different parameters of FWHM (6, 8, 10, 16) , with fixed order 5.

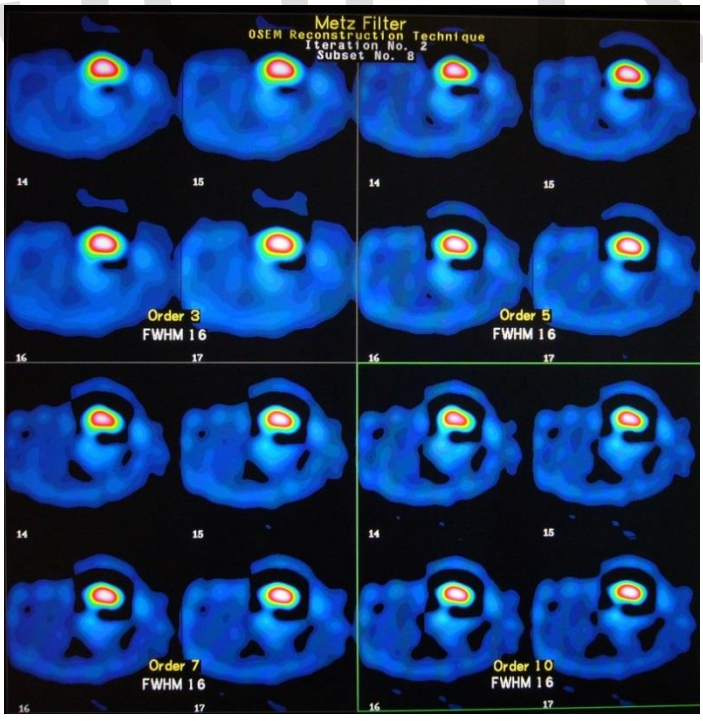

Figure (9) Transverse thyroid frames, reconstructed by OSEM .Metz filter was applied after reconstruction, with four different orders (3, 5, 7, 10), with fixed FWHM 16.

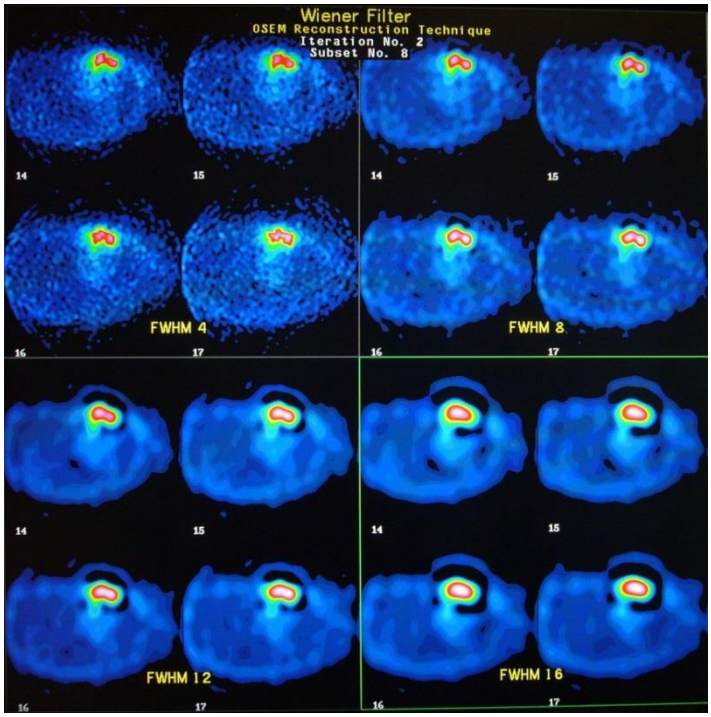

Figure (10) Transverse thyroid frames, reconstructed by OSEM. Wiener filter was applied after reconstruction, with four different parameters of FWHM (4, 8, 12, 16).

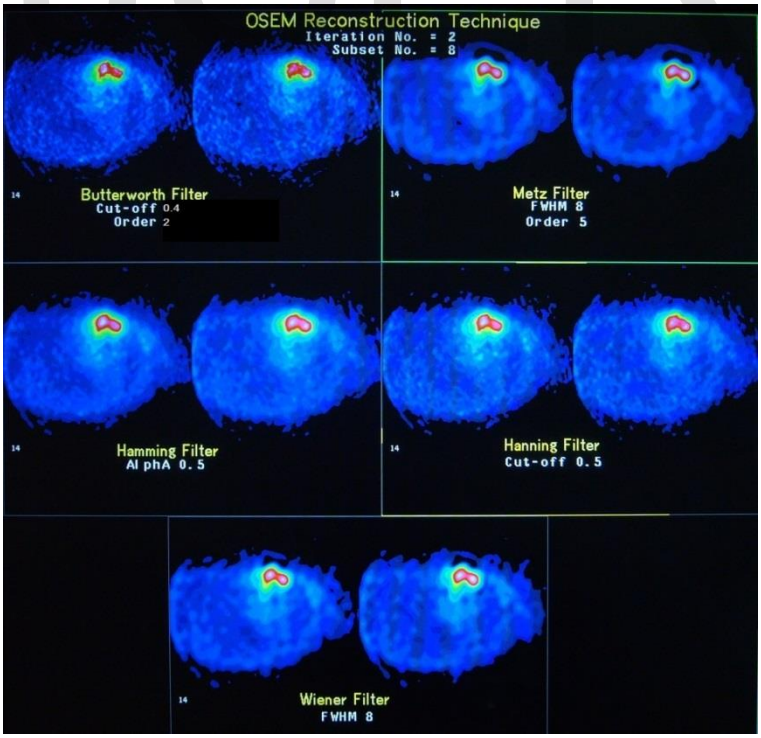

Figure (11) Optimum parameters for different filters used in Thyroid SPECT Imaging.

3.2 Image Analysis:

Calculating image resolution

FWHM expresses image resolution. FWHM was calculated by drawing LSP (line spread function) through origin Pro-lab8 program as described above [6]. The following figures and tables illustrate different values of FWHM for different filter parameters.

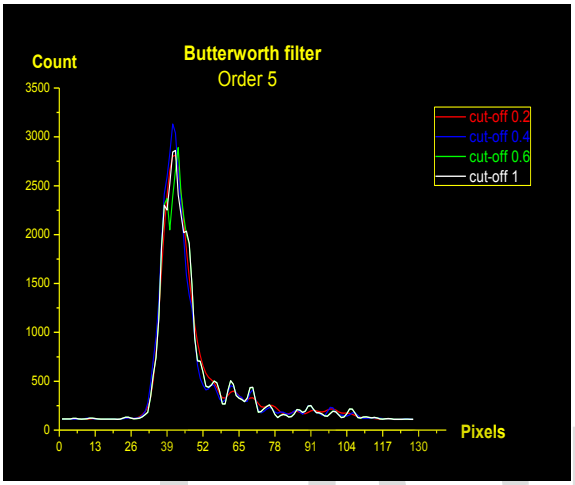

Cut-off (cm^{-1})	FWHM (pixels)
0.2	10.74
0.4	10.01
0.6	11.18
1	10.99

Table (1)

Figure (12) four line profiles representing different values of FWHM after filtering by Butterworth filter using different cut-offs (0.2, 0.4 ,0.6, 1 cm^{-1}), with fixed order 5. Different values of FWHM are shown in **Table (1).**

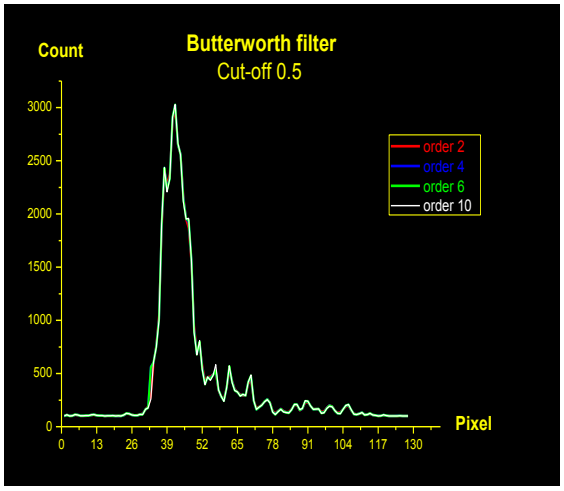

Order	FWHM (pixels)
2	10.79
4	10.9
6	10.89
10	10.75

Table (2)

Figure (13) four line profiles representing different values of FWHM after filtering by Butterworth filter using different orders of (2, 4, 6, 10), with fixed cut-off 0.5 cm^{-1}. Different values of FWHM are shown in **Table (2).**

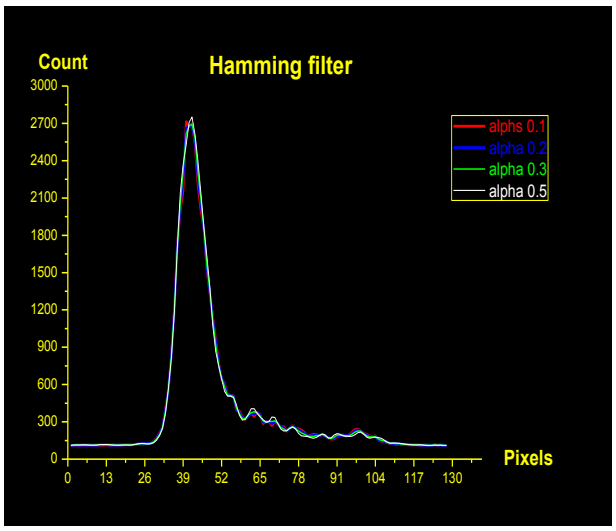

Alpha (cm^{-1})	FWHM (pixels)
0.1	11.3
0.2	11.25
0.3	11.19
0.5	11.07

Table (3)

Figure (14) four line profiles representing different values of FWHM after filtering by Hamming filter using different Alpha parameters (0.1,0.2,0.3,0.5 cm^{-1}). Different values of FWHM are shown in **Table (3).**

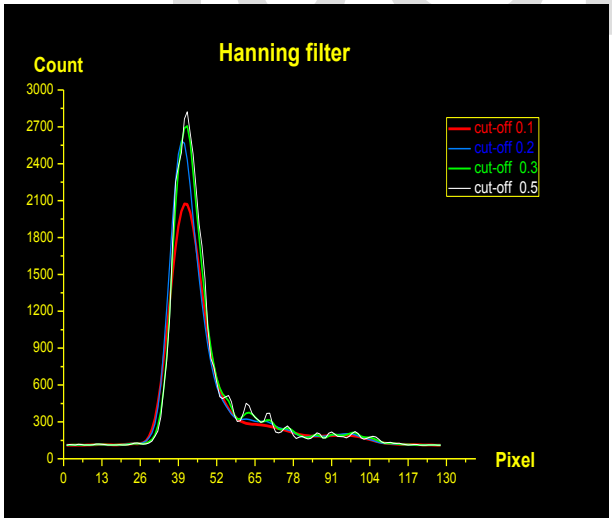

Cut-off (cm^{-1})	FWHM (pixels)
0.1	13.21
0.2	11.43
0.3	11.2
0.5	10.98

Table (4)

Figure (15) four line profiles representing different values of FWHM after filtering by Hanning filter using different cut-offs (0.1, 0.2, 0.3, 0.5 cm^{-1}). Different values of FWHM are shown in **Table (4).**

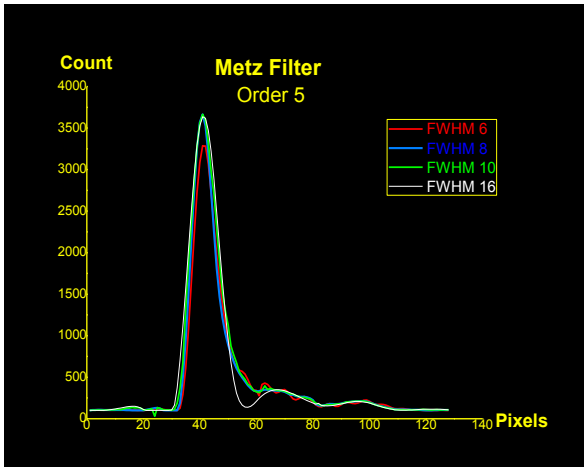

FWHM (of Metz Filter)	FWHM (pixels)
6	9.78
8	9.36
10	10.8
16	11.1

Table (5)

Figure (16) four line profiles representing different values of FWHM after filtering by Metz filter using different FWHM (6, 8, 10, 16), with fixed order 5. Different values of FWHM are shown in **Table (5).**

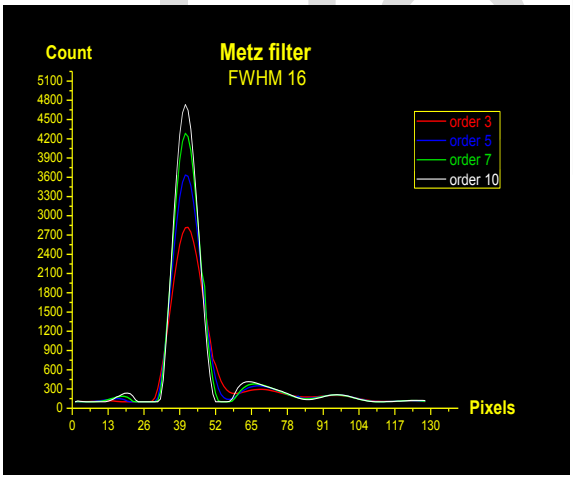

Order	FWHM (pixels)
3	12.5
5	11.09
7	10.34
10	9.52

Table (6)

Figure (17) four line profiles representing different values of FWHM after filtering by Metz filter using different orders (3, 5, 7, 10), with fixed FWHM 16. Different values of FWHM are shown in **Table (6)**

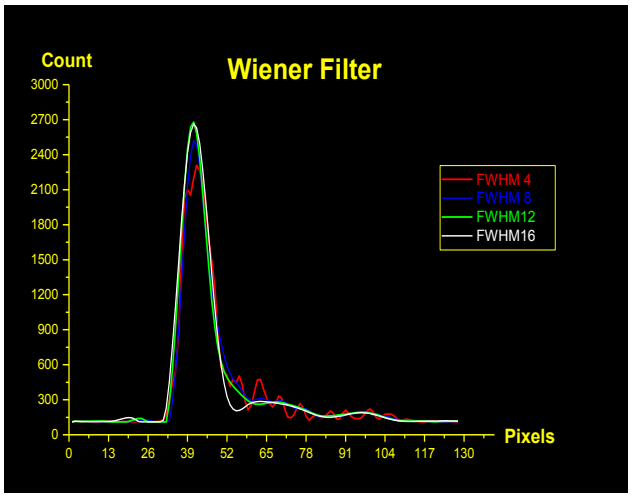

FWHM (of Wiener Filter)	**FWHM** (pixels)
4	10.7
8	9.78
12	9.74
16	10.49

Table (7)

Figure (18) four line profiles representing different FWHM after filtering by Wiener filter with using different FWHM (4, 8, 12, 16). Different values of FWHM are shown in **Table (7).**

Calculating image contrast

Contrast of the image was calculated by using equation (6). The Following table shows different values of contrast after using different filter parameters.

Filter	Parameter of the filter		Contrast %
Butterworth	Cut-off	0.2	86.23
		0.4	86.12
		0.6	86.36
		1	86.35
	Order	2	86.25
		4	86.33
		6	86.39
		10	86.42
Hamming	Alpha	0.1	85.16
		0.2	85.29
		0.3	85.43
		0.5	85.69
Hanning	Cut-off	0.1	79.97
		0.2	84.92
		0.3	85.63
		0.5	85.95
Metz	FWHM	6	88.97
		8	91.55
		10	94.13
		16	96.05
	Order	3	88.41
		5	96.05
		7	98.78
		10	99.43
Wiener	FWHM	4	86.51
		8	89.94
		12	93.91
		16	95.56

Table (8) Different Values of image contrast for different parameters of reconstruction filters.

Calculating image Noise

The mean and SD within the ROI were measured and the Percent root mean square noise (RMS) calculated from the equation (7). The Following table shows different values of RMS% noise after using different filter parameters.

Filter	Parameter of the filter		RMS % (Noise)
Butterworth	Cut-off	0.2	20.97
		0.4	20.89
		0.6	20.95
		1	21.13
	Order	2	20.3
		4	20.7
		6	20.79
		10	20.83
Hamming	Alpha	0.1	21.13
		0.2	20.67
		0.3	20.26
		0.5	19.6
Hanning	Cut-off	0.1	14.45
		0.2	18.28
		0.3	19.59
		0.5	19.83
Metz	FWHM	6	25.86
		8	24.89
		10	23.73
		16	19.06
	Order	3	15.48
		5	19.06
		7	21.98
		10	25.62
Wiener	FWHM	4	23.99
		8	24.93
		12	22.81
		16	20.82

Table (9) Different Values of image RMS% for different parameters of reconstruction filters.

3 Discussion:

The results of this study can have important clinical applications. SPECT filters can affect the quality of the images by their degree of smoothing and noise reduction. Determining the best filter parameters can help to ensure the most accurate diagnosis. Most SPECT filter functions allow the user to control the degree of high frequency suppression with the help of filter parameters. Two important parameters are the "cut-off frequency" and "order or power" of the filter function. The cut-off frequency determines the filter rolling off to a zero gain whereas the rolling off is determined by the order in the filter function. Higher the order, the sharper is the roll off. The location of the cut-off frequency determines how the filter will affect both image noise and resolution. Low cut-off frequency provides good noise suppression, but blurs the images. Higher cut-off frequency can preserve the resolution, but does not suppress noise sufficiently [14].

Spatial resolution (by FWHM), contrast and noise (RMS%) were calculated for transaxial thyroid images which filtered by different parameters of Butterworth, Hamming, Hanning, Metz and Wiener filters. Filtering was applied after reconstruction of images in transaxial direction by OSEM technique.

For **Butterwoth** filter 8 differences were studied as shown in figures (4), (5). The best image resolutions for Butterworth were given by cut-off 0.4 cm^{-1} (with fixed order 5) as shown in table (1) and order 4 (with fixed cut-off 0.5 cm^{-1}) as shown in table (2). From table (8) we notice that image contrast slightly improves with higher cut-offs and higher orders. Noise also slightly increases with higher cut-offs and orders. Butterworth is noticed to retain suitable level of changes in image noise. The adequate parameters for using Butterworth filter are cut-offs (0.2, 0.4 cm^{-1}) and orders (2, 4).

For **Hamming** filter 4 differences were studied as shown in figure (6). The best image resolution was given by alpha 0.1 cm^{-1} as shown in table (3). In Hamming the resolution doesn't greatly changed with different changes of alpha. Image contrast slightly improves with higher values of alpha as shown in table (8). Image noise reduction was improved with higher values of alpha, therefore the adequate parameter for using Hamming filter is alpha 0.5 cm^{-1} due to the lower value of image noise.

For **Hanning** filter 4 differences were studied as shown in figure (7). The best image resolution was given by cut-off 0.5 cm^{-1} as shown in table (4). Image contrast is improved with higher cu-offs as shown in table (8). On the contrary of Hamming filter, image noise increases with higher cut-offs as shown in table (9). The aedquate parameters for using Hanning filter are cut-off s 0.3 and 0.5 cm^{-1}. Hamming and Hanning filters are very effective and better than other filters in reducing image noise. As shown in table (9) the lower values of noise is given by filtering with Hamming and Hanning filters. Despite of improving noise reduction in these two filters, spatial resolution of the images are lower than other filters (increasing FWHM means decreasing resolution). The lower the resolution and contrast at lower cut-offs, the lower sharpness of the images and more blurring with diffused details as shown in figure (7).

For **Metz** filter 8 differences were studied as shown in figures (8),(9) .The best image resolutions was given by FWHM 6 (with fixed order 5) as shown in table (5) and order 10 (with fixed FWHM 16) as shown in table (6). Image resolution is decreased with higher values of FWHM of Metz filter and slightly improved with higher orders. Image contrast improves greatly with higher values of filter FWHM and higher orders as shown in table (8). Metz filter shows the higher image contrast values over the other filters. Image noise reduction improves with higher FWHM and decreases with higher orders as shown in table (9). From results, images filtered with Metz contain more noise than the other images. According to decreased resolution and more noise with higher FWHM of Metz the image is more burring and the details are overlapped as shown in figure(8). The same blurred images with less details appear with

higher orders due to increasing noise as shown in figure (9). The adequate parameters for using Metz filter are FWHM 6, 8 (with order 5).

For **Wiener** filter 4 differences were studied as shown in figure (10). The best image resolutions were given by FWHM 8 and 12 as shown in table (7). Image resolution started to decrease with FWHM higher than 8. Image contrast improves with higher FWHM as shown in table (8). Image noise reduction slightly improves with FWHM higher than 8 as shown in table (9).The adequate filter parameter used with Wiener is FWHM 8.

From results of this research the optimum parameters of filters which can be used in Thyroid SPECT image analysis after OSEM reconstruction are shown in figure (11) and the following table (10).

Filter	**Optimum Parameter of the filter**		
Butterworth	Cut-off	0.2	0.4
	Order	2	4
Hamming	Alpha	0.5	
Hanning	Cut-off	0.5	
Metz	FWHM	6	8
	Order	5	
Wiener	FWHM	8	

Table (10) the optimum parameters of filters which can be used in Thyroid SPECT image analysis after OSEM reconstruction.

Our study agrees with **Zaidi**, who used order 3 and cut-off of 0.4 cm-1for Butterworth filter. Images were obtained in transaxial direction after Thyroid imaging by SPECT [15].

Our study also agrees with Thyroid volume estimations were performed by **Van Isselt** et al., in patients with Graves' disease. With SPECT, the iteratively reconstructed thyroid images were filtered and for noise reduction, a 3D edge preserving 3×3×3-point median filter was applied [16].

Also our study agree with **Bahk** et al., who used an acrylic thyroid phantom in their study for pinhole SPECT imaging in normal and morbid ankles. The phantom was subjected to planar, SPECT and pinhole SPECT acquisitions. The gamma camera system was connected to an Icon data processor that enabled image reconstruction using the FBP algorithm and a Butterworth filter. The FBP algorithm and a Butterworth filter were used for reconstruction as in the phantom study [17].

4 Conclusion:

One of the most important factors that greatly affect the quality of clinical SPECT images is image filtering. Image filtering is a smoothness process for noise removal and resolution recovery. A number of filters have been designed and are available in the reconstruction of tomographic image. The same filter with different parameters can affect variously the image quality. The type of the filter and the application of the filter parameters cannot be generalized in all types of clinical SPECT studies. The selection of the optimal filter and the determination of filter parameters for any individual case remains one of the main problems of filtering in SPECT image processing. Therefore, the filters parameters must be standardized before being put to clinical use.

In this research parameters of five filters (low-pass filters) were optimized to produce more accurate images with high quality and better physical characteristics of resolution, contrast and noise. Therefore, results in this research can help physicians and researchers in nuclear medicine in case of thyroid SPECT imaging especially by gamma camera with parallel-hole collimator.

5 References:

1. Bruyant, P. P. (2002). Analytic and iterative reconstruction algorithms in SPECT. Journal of Nuclear Medicine, 43(10), 1343-1358.

2. Zeng, G. L. (2001). Image reconstruction—a tutorial. Computerized medical imaging and graphics, 25(2), 97-103.

3. Tsui, B. M. (1996). The AAPM/RSNA physics tutorial for residents. Physics of SPECT. Radiographics, 16(1), 173-183.

4. Lyra, M., & Ploussi, A. (2011). Filtering in SPECT image reconstruction. International Journal of Biomedical Imaging, 2011.

5. Gilland, D. R., Tsui, B. M., McCartney, W. H., Perry, J. R., & Berg, J. (1988). Determination of the optimum filter function for SPECT imaging. Journal of nuclear medicine, 29(5), 643-650.

6. Khalil, M. (Ed.). (2010). Basic sciences of nuclear medicine. Springer Science & Business Media.

7. SALIHIN, Y. M., & Zakaria, A. (2009). Determination of the optimum filter for qualitative and quantitative 99mTc myocardial SPECT imaging.

8. King, M. A., Glick, S. J., Penney, B. C., Schwinger, R. B., & Doherty, P. W. (1987). Interactive visual optimization of SPECT pre-reconstruction filtering. J Nucl Med, 28(7), 1192-1198.

9. King, M. A., Schwinger, R. B., Doherty, P. W., & Penney, B. C. (1984). Two-dimensional filtering of SPECT images using the Metz and Wiener filters. Journal of Nuclear Medicine, 25(11), 1234-1240.

10. Links, J. M., Jeremy, R. W., Dyer, S. M., Frank, T. L., & Becker, L. C. (1990). Wiener filtering improves quantification of regional myocardial perfusion with thallium-201 SPECT. Journal of nuclear medicine: official publication, Society of Nuclear Medicine, 31(7), 1230-1236.

11. Van Laere, K., Koole, M., Lemahieu, I., & Dierckx, R. (2001). Image filtering in single-photon emission computed tomography: principles and applications. Computerized Medical Imaging and Graphics, 25(2), 127-133.

12. Cherry, S. R., Sorenson, J. A., & Phelps, M. E. (2012). Physics in nuclear medicine e-Book. Elsevier Health Sciences.

13. Leong, L. K., Kruger, R. L., & O'connor, M. K. (2001). A comparison of the uniformity requirements for SPECT image reconstruction using FBP and OSEM techniques. Journal of nuclear medicine technology, 29(2), 79-83.

14. Pandey, A. K., Pant, G. S., & Malhotra, A. (2004). Standardization of SPECT filter parameters. Indian Journal of Nuclear Medicine, 19(2), 30-35.

15. Zaidi, H. (1996). Comparitive methods for quantifying thyroid volume using planar imaging and SPECT. The Journal of Nuclear Medicine, 37(8), 1421.

16. van Isselt, J. W., de Klerk, J. M., van Rijk, P. P., van Gils, A. P., Polman, L. J., Kamphuis, C., ... & Beekman, F. J. (2003). Comparison of methods for thyroid volume estimation in patients with Graves' disease. European journal of nuclear medicine and molecular imaging, 30(4), 525-531.

17. Bahk, Y. W., Chung, S. K., Young-Ha, P., Sung-Hoon, K., & Hyoung-Koo, L. (1998). Pinhole SPECT imaging in normal and morbid ankles. The Journal of Nuclear Medicine, 39(1), 130.